J Nanostruct 16(3): 3201-3206, Summer 2026

RESEARCH PAPER

Preparation and Characterization of Nanoscale $BaTiO_3$

Anas A. Hamdi, Mohammed A. Mohmmed *

Salahuddin Education Directorate, Ministry of Education, Salahuddin, Iraq

ARTICLE INFO

Article History:
Received 05 March 2026
Accepted 13 May 2026
Published 01 July 2026

Keywords:
$BaTiO_3$
Hydrothermal treatment
Nanoscale
SEM
XRD

ABSTRACT

In this work, a 1:1 molar ratio of TiO_2 and barium salts was used to prepare a $BaTiO_3$ nanocomposite. A precursor solution was prepared through the chemical precipitation method and then hydrothermally treated to achieve different morphologies and structural forms of the nanocomposite. X-ray diffraction, which was used for structural characterization, demonstrated that the nanocomposite had an average particle size of approximately 56 nm and validated its crystalline nature. Surface morphology and particle size were assessed through scanning electron microscopy. The elemental composition and weight percentages of constituent elements were also determined by employing energy-dispersive X-ray spectroscopy to confirm the effective synthesis of the nanocomposite. These results were then compared with the anticipated theoretical values.

How to cite this article
Hamdi A., Mohmmed M. Preparation and Characterization of Nanoscale $BaTiO_3$. J Nanostruct, 2026; 16(3):3201-3206.
DOI: 10.22052/JNS.2026.03.016

INTRODUCTION

Hydrothermal synthesis is the best approach for regulating the properties of samples under varying synthesis conditions, and all of the various forms aid in further enhancing the necessary qualities to make the samples suitable for different applications [1,2]. The working process of the hydrothermal synthesis reaction comprises two components. The initial step involves breaking down the source material into an ionic form by dissolving it in a particular solvent [3, 4]. Crystallization occurs when the raw material is at its most soluble, and the outcome of this phenomenon provides the finished product its strength [5]. $BaTiO_3$ is a common electrical ceramic material that can be employed at normal temperatures [6]. It has a tetragonal perovskite lattice structure and is a pure material that changes from an electrical state to a semielectric cubic state at the Curie temperature Tc or approximately 130 °C [7,8]. Undoped $BaTiO_3$ is an electrical insulator, and oxygen deficiency occurs at high temperatures ($BaTiO_3$ > T) in air (in degrees Celsius) or in a reducing atmosphere [9]. Extensive research has been conducted on the use of $BaTiO_3$ nanoparticles in dynamic random access memory, photovoltaic devices, and multilayer ceramic capacitors (MLCCs) [10] because of their high dielectric constant and photovoltaic properties [11]. The production of microelectronic devices uses $BaTiO_3$ nanoparticles, a type of nanomaterial. Additionally, MLCCs are made with $BaTiO_3$ nanoparticles [12]. The resultant material has special cohesive and preservation qualities. Barium nanoparticles affect ferroelectricity and have a precise size. [13]. Techniques used to create barium nanoparticles include wet chemical

* *Corresponding Author Email: Mohmmed.ab.mohmmed@st.tu.edu.iq*

processing, traditional solid-state processes, and homogeneous organization via calcination at temperatures higher than 700 °C. Controlling the size and shape of structures, electronics, and systems at the nanoscale level (1–100) is known as nanotechnology [14]. Nanoparticles, with a diameter of less than 100 nm, have generated considerable attention and controversy and experienced increased utilization in a number of industrial domains [15]. Numerous reports on the effective hydrothermal synthesis of $BaTiO_3$ with enhanced characteristics exist. Wang et al. (2012) investigated the mechanism underlying the transformation from TiO_2 to $BaTiO_3$ under hydrothermal conditions to gain insight into the dynamics of nucleation and growth [16]. Chen et al. (2016) fabricated lead-free $BaTiO_3$-based ceramics with improved piezoelectric performance by optimizing hydrothermal synthesis conditions [17].

MATERIALS AND METHODS

Preparation of Nanoscale $BaTiO_3$

$BaTiO_3$ nanoparticles were produced through a hydrothermal method employed in the United States (U.S.) by using $Ba(OH)_2{\cdot}8H_2O$); U.S.-based TiO_2 (rutile or anatase); deionized water; NaOH for pH adjustment; a sprinkling stainless steel autoclave lined with Teflon; a filter or centrifuge; and a lab oven set at 250 °C. Ethanol or acetone was utilized for washing.

Method steps

1. Preparation of the solution: Stir and dissolve stoichiometric $Ba(OH)_2{\cdot}8H_2O$ in deionized water. Add the TiO_2 powder while aggressively stirring.

2. Optional pH adjustment: If required, add NaOH to increase alkalinity for improved crystallization.

3. Hydrothermal treatment: Place the mixture in an autoclave lined with Teflon. Warm to 180

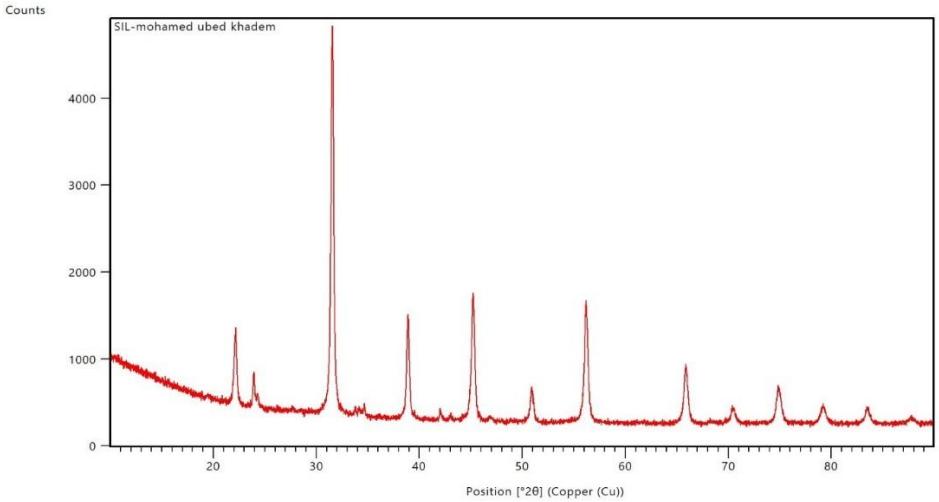

Fig. 1. XRD spectra of nanoscale $BaTiO_3$ synthesized through the hydrothermal method.

Table 1. Representative Miller indices.

hkl	I%	d-A	2θ
100	Medium	3.99	22.2
110	Strong	2.84	31.5
111	Medium	2.31	38.8
200	Strong	2.00	45.3
210	Medium	1.80	50.8
300	Weak	1.34	70.2

°C–220 °C for 12–24 h to enable the production of nanoparticles under intense pressure.

The autoclave should be allowed to naturally cool to ambient temperature.

4. Product collection: Remove the autoclave and collect the white precipitate. Clean using ethanol and deionized water. Centrifugation or filtration can be used to separate the product.

5. Drying: Bake the cleaned product at 60 °C–80 °C for several hours.

6. Calcination: Calcinate for 2–4 h at 600 °C to improve crystallinity and eliminate residue.

$BaTiO_3$ is a fine, white nanopowder that ranges in size from 20 nm to 100 nm depending on synthesis conditions. Final tests for characterization included X-ray diffractometry (XRD), scanning electron

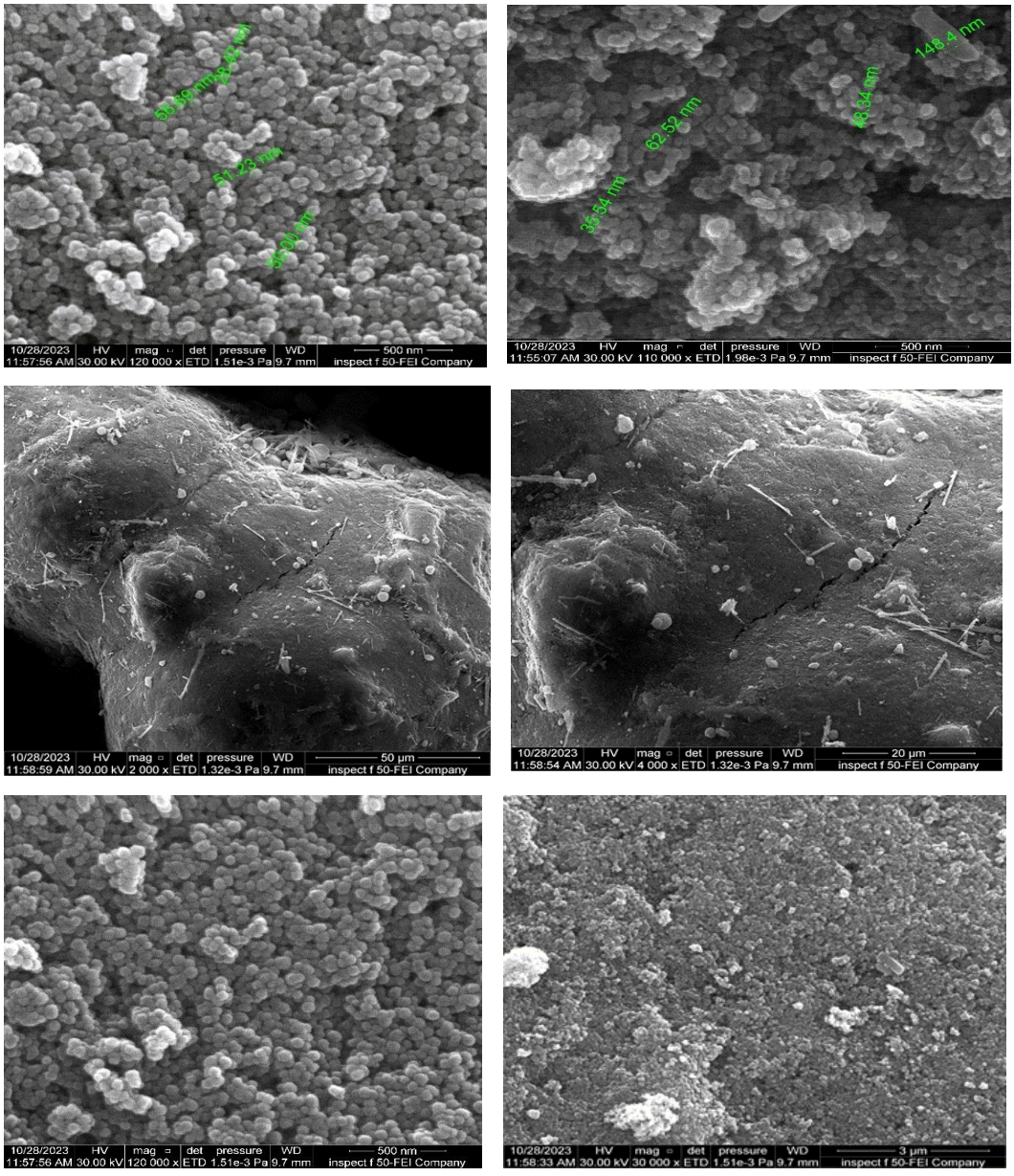

Fig. 2. SEM images of nanoscale $BaTiO_3$ nanopowder prepared through the hydrothermal method under different magnifications.

microscopy (SEM), and energy-dispersive X-ray spectroscopy (EDX).

RESULTS AND DISCUSSION

The XRD pattern of nanoscale $BaTiO_3$ produced through the hydrothermal method is displayed in Fig. 1. The XRD pattern seen in Fig. 1 attests to the crystalline structure of the produced $BaTiO_3$ nanoparticles. High crystallinity is indicated by strong and prominent peaks. The successful production of the target phase is confirmed given that the peak positions are in good agreement with those in the typical diffraction pattern of cubic or tetragonal perovskite $BaTiO_3$. Considering the absence of visible impurity peaks, the product is a pure phase. As is typical of the (110) plane of $BaTiO_3$, the strongest peak arises at approximately $2\theta \approx 31°$. Additional noteworthy peaks matching known crystallographic planes of the perovskite structure support the effective synthesis of nanoscale $BaTiO_3$. Peak splitting in tetragonal $BaTiO_3$ occurs close to $2\theta = 45°$ and 65° because of anisotropic lattice constants ($a \neq c$). Single symmetric peaks ($a = b = c$) are present in cubic $BaTiO_3$. The presence of the intended phase is confirmed when these peaks are compared with those in typical JCPDS cards (such as No. 05-0626). Broadened peaks imply particle sizes on the nanoscale, whereas sharp peaks indicate high crystallinity. Crystallite size is calculated by applying the [18] Scherrer equation below:

$$D = (k\lambda)/(\beta \cos\theta)$$

where is the form factor (≈0.9), D is the size of the crystallite, λ is the X-ray wavelength (1.5406 Å for Cu Kα), β is the full width at half maximum in radians, and θ is the Bragg angle. Wide XRD

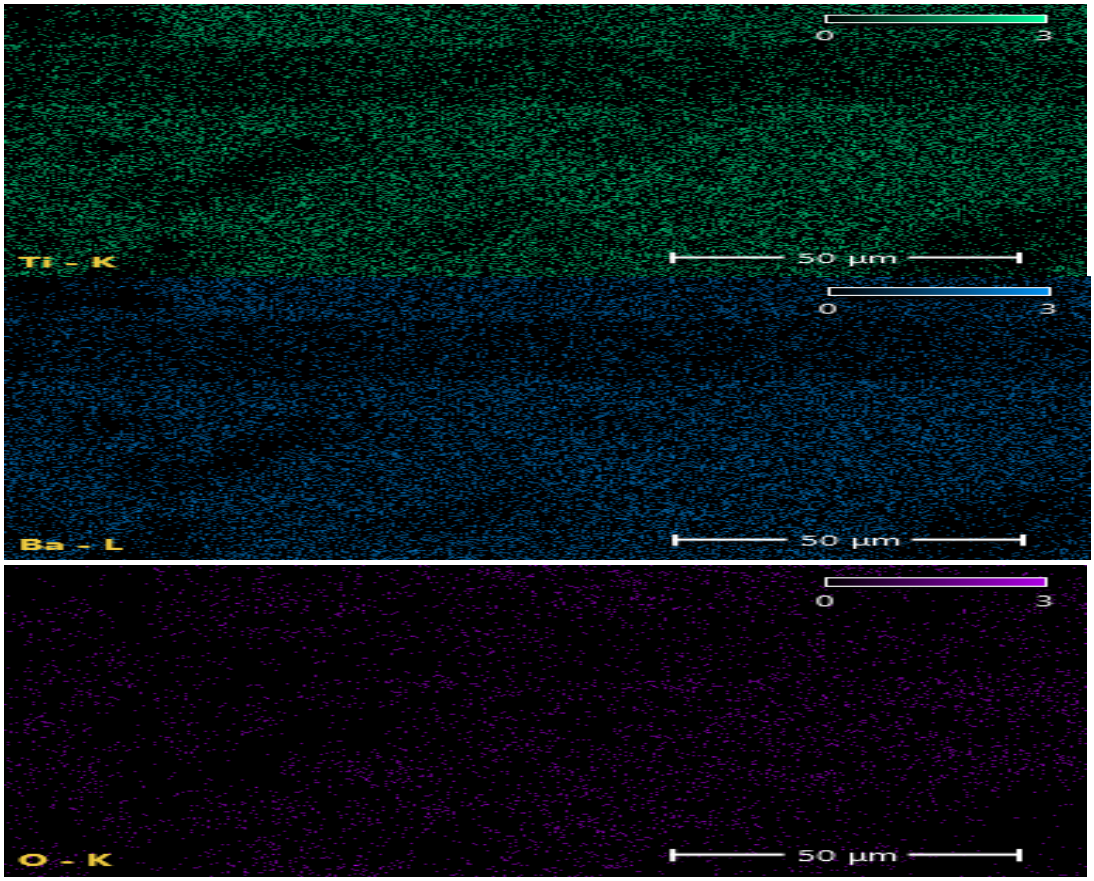

Fig. 3. EDX images of $BaTiO_3$ prepared through the hydrothermal technique. Various colors indicate compounds with the O element.

peaks indicate small crystal sizes that are usually between 20 and 65 nm.

Analysis of $BaTiO_3$ Nanoparticles via SEM

Fig. 2 evidently shows that the nanoparticles are usually spherical, quasispherical, or pseudocubic in shape. Their edges may be faceted or smooth depending on the synthesis conditions and crystallinity. Naturally occurring agglomeration may cause some particles to group together. Spherical or pseudocubic shapes signify a uniform and regulated crystal formation, which is frequently achieved under appropriate hydrothermal conditions. On average, particles should be between 56 and 68 nm in size. Size was estimated on the basis of the SEM scale bar. Unexpectedly large particles could be a sign of inadequate dispersion or agglomeration. Uniformly small particle sizes indicate regulated crystal formation and efficient nucleation during hydrothermal synthesis. van der Waals forces and surface energy cause nanoparticles to tend to aggregate. In the SEM image, agglomerates may appear as irregular forms or dense clusters. Poor synthesis is not always the cause of agglomeration, which is common. Using dispersants or surfactants can typically reduce agglomeration. The homogeneous distribution of particles across the image indicates good dispersion and constant synthesis conditions. Inhomogeneity could indicate temperature gradients throughout the process, inadequate mixing, or an imbalance in pH. A homogeneous image verifies consistent particle production and repeatability across the sample. Semispherical $BaTiO_3$ nanoparticles with an average particle size of approximately 50 nm are visible in the SEM image. Although high surface energy causes the particles to clump together, their homogeneous morphology shows that in accordance with [19], the hydrothermal synthesis was successful. The image suggests good crystallinity and size distribution.

EDX Analysis

Fig. 3 illustrates the EDX spectra of the $BaTiO_3$ nanoparticles. EDX was conducted to determine the elemental makeup of the produced $BaTiO_3$ nanoparticles. EDX is usually performed in

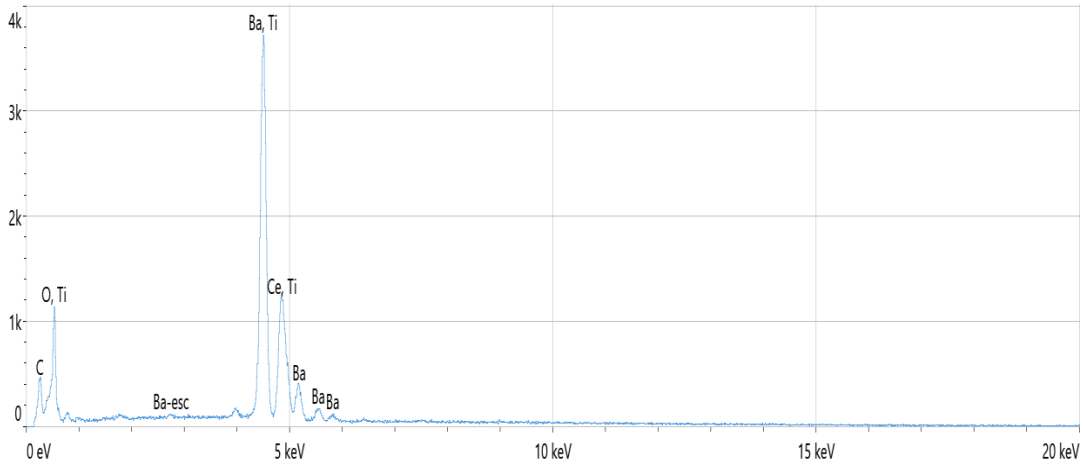

Fig. 4: EDX spectra of $BaTiO_3$.

Table 2. Elemental weight percentage and atomic percentage provided by EDX software. The approximate atomic ratio for stoichiometric $BaTiO_3$ should be close.

Element	Atomic %	Atomic % Error	Weight %	Weight % Error
O	66.8	1.1	25.1	0.4
Ti	15.3	0.4	17.2	0.4
Ba	17.9	0.3	57.7	0.8

conjunction with SEM. The following components constitute the optimal $BaTiO_3$ compound: O, Ti, and Ba. Additional peaks can be a sign of impurities (from contamination or precursors), residues (such as C from sample preparation or coating), and substrate elements (such as Si if on a silicon wafer). The presence of the key peaks Ba Lα or Mα (~4.5–5.2 keV) verifies that Ba has been incorporated into the perovskite lattice and is present. Ti Kα (~4.5 keV) verifies that Ti is present in the anticipated oxidation state. Given that O Kα (~0.5 keV) corresponds to oxygen, the compound's oxide structure is confirmed to be in conformity with that reported in [20]. Fig. 4 shows EDX spectra of powdered $BaTiO_3$ prepared through a hydrothermal process.

CONCLUSION

1. The XRD pattern confirmed the formation of perovskite $BaTiO_3$. Peak splitting is an important indicator of the tetragonal phase. Wide peaks suggest a nanocrystalline structure. A good match with JCPDS demonstrates that the intended structure was successfully synthesized. These observations corroborate the XRD results for the crystalline structure of the $BaTiO_3$ powder and validate its nanoscale nature.

2. SEM images of the produced $BaTiO_3$ nanoparticles reveal a homogeneous shape with abundant spherical or polyhedral particles. The successful production of the nanomaterial is indicated by the observed particle size, which is in the nanometer range (between 50 and 100 nm). Given their high surface energy, nanomaterials frequently exhibit some degree of agglomeration. The particles' smooth and thick surface suggest good crystallinity and consistent development throughout the hydrothermal process.

3. The presence of O, Ti, and Ba peaks in EDX spectra indicates that $BaTiO_3$ was successfully formed. The absence of unanticipated components suggests excellent purity. Atomic ratios close to the expected stoichiometry support proper synthesis.

CONFLICT OF INTEREST

The authors declare that there is no conflict of interests regarding the publication of this manuscript.

REFRENCES

1. Kumar P, Kumar R. Synthesis process of functionalized ZnO nanostructure for additive manufacturing: a state-of-the-art review. Additive Manufacturing with Functionalized Nanomaterials: Elsevier; 2021. p. 135-153.
2. Sun W, Li J. Microwave-hydrothermal synthesis of tetragonal barium titanate. Mater Lett. 2006;60(13-14):1599-1602.
3. Wu SY, Chen XM, Yu HY. Hydrothermal synthesis of $Ba_5Nb_4O_{15}$ ultrafine powders. J Eur Ceram Soc. 2006;26(10-11):1973-1976.
4. Ai PF, Li WY, Xiao LY, Li YD, Wang HJ, Liu YL. Monodisperse nanospheres of yttrium oxysulfide: Synthesis, characterization, and luminescent properties. Ceram Int. 2010;36(7):2169-2174.
5. Kato K, Mimura K-i, Dang F, Imai H, Wada S, Osada M, et al. $BaTiO_3$ nanocube and assembly to ferroelectric supracrystals. J Mater Res. 2013;28(21):2932-2945.
6. Haertling GH. Ferroelectric Ceramics: History and Technology. J Am Ceram Soc. 1999;82(4):797-818.
7. Capurso JS, Alles AB, Schulze WA. Processing of Laminated Barium Titanate Structures for Stress-Sensing Applications. J Am Ceram Soc. 1995;78(9):2476-2480.
8. Dutta PK, Asiaie R, Akbar SA, Zhu W. Hydrothermal Synthesis and Dielectric Properties of Tetragonal BaTiO3. Chem Mater. 1994;6(9):1542-1548.
9. Hakuta Y, Ura H, Hayashi H, Arai K. Continuous Production of $BaTiO_3$ Nanoparticles by Hydrothermal Synthesis. Industrial and Engineering Chemistry Research. 2005;44(4):840-846.
10. Lee SK, Park TJ, Choi GJ, Koo KK, Kim SW. Effects of KOH/BaTi and Ba/Ti ratios on synthesis of BaTiO3 powder by coprecipitation/hydrothermal reaction. Mater Chem Phys. 2003;82(3):742-749.
11. Beauger A, Mutin JC, Niepce JC. Synthesis reaction of metatitanate BaTiO3. Journal of Materials Science. 1983;18(12):3543-3550.
12. Alfareed TM, Slimani Y, Almessiere MA, Nawaz M, Khan FA, Baykal A, et al. Biocompatibility and colorectal anti-cancer activity study of nanosized BaTiO3 coated spinel ferrites. Scientific Reports. 2022;12(1).
13. Fakhar-e-Alam M, Saddique S, Hossain N, Shahzad A, Ullah I, Sohail A, et al. Synthesis, Characterization, and Application of BaTiO3 Nanoparticles for Anti-Cancer Activity. J Cluster Sci. 2022;34(4):1745-1755.
14. Yoon YN, Lee D-S, Park HJ, Kim J-S. Barium Titanate Nanoparticles Sensitise Treatment-Resistant Breast Cancer Cells to the Antitumor Action of Tumour-Treating Fields. Scientific Reports. 2020;10(1).
15. Genchi GG, Marino A, Rocca A, Mattoli V, Ciofani G. Barium titanate nanoparticles: promising multitasking vectors in nanomedicine. Nanotechnology. 2016;27(23):232001.
16. Wang Y-Z. Hydrothermal Synthesis Nano Mg-Al LDHs and its Formation Mechanism. Journal of Inorganic Materials. 2008;23(1):93-98.
17. Beltrán H, Cordoncillo E, Escribano P, Sinclair DC, West AR. Insulating Properties of Lanthanum-Doped $BaTiO_3$ Ceramics Prepared by Low-Temperature Synthesis. J Am Ceram Soc. 2004;87(11):2132-2134.
18. Shah AA, Khan A, Dwivedi S, Musarrat J, Azam A. Antibacterial and Antibiofilm Activity of Barium Titanate Nanoparticles. Mater Lett. 2018;229:130-133.
19. Farhan FK, Mawat MM, Odah JF. Effect of Bone Protein addition to the system: Calcium Titanate. Physics and Chemistry of Solid State. 2024;25(4):880-884.
20. Farhan FK, Kadhim MO, Ashour SJ. Preparation and Development of Ceramic System $CaTiO_3$ for Used Medical Applications. Journal of Computational and Theoretical Nanoscience. 2019;16(1):109-114.